High-resolution electron-beam-induced-current study of the defect structure in GaN epilayers

2002 J. Phys.: Condens. Matter 14 13285

(http://iopscience.iop.org/0953-8984/14/48/379)

INSTITUTE OF PHYSICS PUBLISHING JOURNAL OF PHYSICS: CONDENSED MATTER

J. Phys.: Condens. Matter **14** (2002) 13285–13290 PII: S0953-8984(02)53986-2

High-resolution electron-beam-induced-current study of the defect structure in GaN epilayers

N M Shmidt[1], O A Soltanovich[2], A S Usikov[1], E B Yakimov[2] and E E Zavarin[1]

[1] Ioffe Physico-Technical Institute, RAS, 26 Polytekhnicheskaya Str., St Petersburg, 194021, Russia
[2] Institute of Microelectronics Technology, RAS, Chernogolovka, 142432, Russia

E-mail: yakimov@ipmt-hpm.ac.ru

Received 27 September 2002
Published 22 November 2002
Online at stacks.iop.org/JPhysCM/14/13285

Abstract

Electron-beam-induced-current (EBIC) investigations of GaN structures grown by metal–organic chemical vapour deposition on (0001) sapphire substrates have been carried out. It is shown that the widths of the EBIC profiles for individual extended defects can be as small as about 100 nm. This width is observed to decrease with decreasing diffusion length and/or with increasing electron beam energy. The high spatial resolution is explained by the small diffusion length in the samples under study. The diffusion length is small even in structures with dislocation densities of about 10^8 cm^{-3} and carrier mobilities of about 600 cm^2 V^{-1} s^{-1} at 300 K and 1800 cm^2 V^{-1} s^{-1} at 125 K.

1. Introduction

The electron-beam-induced-current (EBIC) mode of the scanning electron microscope is now widely used for the characterization of electrically active extended defects in semiconductors and semiconductor structures [1, 2]. As shown by Donolato [3], the full width at half-maximum (FWHM) of the dislocation EBIC contrast in bulk semiconductor crystals is mainly determined by the generation region dimensions and is practically independent of the minority carrier diffusion length. In thin semiconductor layers the FWHM should decrease [4] and could be smaller than the electron range R. A similar decrease could be expected in semiconductor material with a small diffusion length. In the present paper it is demonstrated that individual extended defects with a density exceeding 10^9 cm^{-3} can be revealed in GaN epitaxial layers by EBIC measurements. It is shown that the FWHM does indeed decrease with decreasing diffusion length or increasing primary electron energy. The high spatial resolution achieved is explained by taking into account the submicron diffusion length values in the layers studied.

0953-8984/02/4813285+06$30.00

2. Experimental details

GaN epitaxial layers grown by metal–organic chemical vapour deposition (MOCVD) on (0001) sapphire substrates at a pressure of 200 mbar have been studied. The layers have n-type conductivity with a carrier concentration of (1–20) $\times$ 10^{16} cm^{-3} and a thickness of about 3 μm. Due to different buffer-layer growth conditions, the charge carrier mobility at 300 K and the dislocation density range from 100 to 600 cm^2 V^{-1} s^{-1} and from 10^8 to 3 $\times$ 10^9 cm^{-2}, respectively.

The dislocation density was estimated from x-ray diffractometry data, by measuring the angular distribution of the x-ray diffraction which corresponded to the (0002), (0004), (1010), (2020), and (1124) reflections. Measurements were carried out by means of triple-crystal differential diffractometry with Mo Kα_1 and Cu Kα_1 radiation under conditions of symmetrical and asymmetrical Bragg and Laue geometry.

The main part of the experiments was carried out on two structures labelled A and B. The first has a carrier concentration of about 10^{16} cm^{-3} and a Hall mobility μ of about 600 cm^2 V^{-1} s^{-1} at 300 K and 1800 cm^2 V^{-1} s^{-1} at 125 K, with the temperature dependence of μ typical for high-quality GaN crystals [5]. The second structure (B) has a carrier concentration of about 10^{17} cm^{-3} and μ decreasing from 200 cm^2 V^{-1} s^{-1} at 300 K down to 80 cm^2 V^{-1} s^{-1} at 100 K. The deep-level defect centres in the samples were studied by deep-level transient spectroscopy (DLTS). The Schottky barriers for the EBIC and DLTS measurements were formed by evaporation of a thin layer of Ni/Au. For the two structures, the DLTS measurements revealed the presence of similar deep-level centres, typical for GaN layers grown by the MOCVD method [6, 7]. The EBIC measurements were carried out at room temperature with the scanning electron microscope JSM-840A (Jeol) using the Keithley 428 current amplifier. The diffusion length in the samples studied was estimated from measurement of the dependence of the minority carrier collection efficiency on the electron beam energy E_b. Individual recombination defects were characterized by the contrast value $C(r) = 1 - I_c(r)/I_{c0}$, where $I_c(r)$ and I_{c0} are the collected current values measured with the electron beam located at point r near the defect and far from it, respectively.

3. Results and discussion

Typical EBIC images of the samples under study are presented in figure 1. It is seen that the defect structure in sample A (figure 1(a)) consists mainly of a large number of individual recombination defects with a density of about (2–3) $\times$ 10^8 cm^{-2} with a rather inhomogeneous background. The density of these defects is close to the threading dislocation density estimated for this structure from x-ray diffractometry and atomic force microscopy images, which allows one to associate these defects with threading dislocations and/or small dislocation clusters. The EBIC images of the same region obtained under conditions of zero applied bias (figure 2(a)) and with a reverse bias of 1 V (figure 2(b)) confirm this assumption. In fact, the defect structures obtained under different bias conditions are very similar, although, according to our C–V measurements, the first image corresponds to a depth of about 0.3 μm from the surface while the second one corresponds to a depth of about 0.5 μm. The similarity of these images allows us to conclude that the defects are elongated in the direction perpendicular to the surface. Most of the defects revealed in structure A have similar contrast (about 0.1) and we associated these defects with individual dislocations. The defects with the higher contrast can be associated with small dislocation clusters or dislocation–precipitate clusters. The role of threading dislocations as non-radiative recombination centres was evidenced also in other studies (see e.g. [8]); this correlates well with the assumption that the recombination defects observed in the present study are threading dislocations.

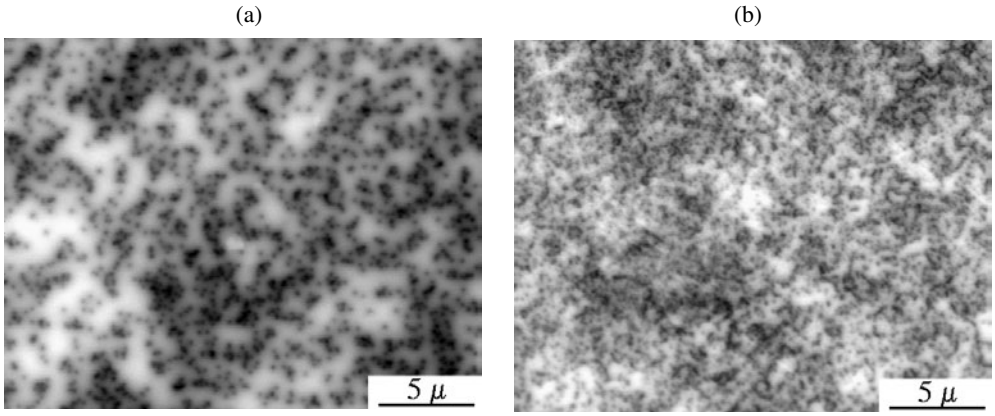

Figure 1. EBIC images of structures A (a) and B (b); $E_b = 35$ keV, $I_b = 3 \times 10^{-10}$ A.

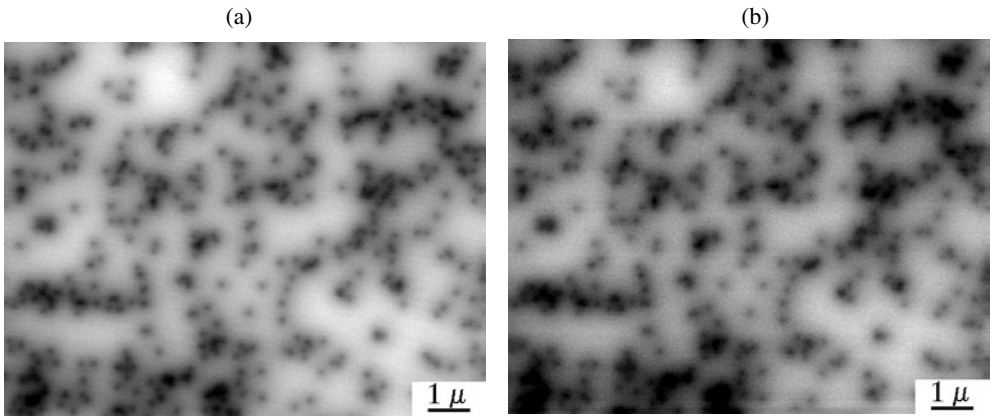

Figure 2. EBIC images of recombination defects in structure A obtained at reverse biases 0 (a) and 1 V (b); $E_b = 35$ keV, $I_b = 3 \times 10^{-10}$ A.

The density of recombination defects in structure B is appreciably higher (figure 1(b)) and reaches (1–2) $\times$ 10^9 cm^{-2}. In the image obtained with the highest resolution (figure 3), defects similar to those present in structure A and with very close contrast values can be also revealed. However, the number of such defects is rather small and most of them have a larger size and higher contrast. This could be explained under the assumption that the majority carrier recombination defects in this structure are dislocation clusters or dislocation–precipitate clusters, although individual threading dislocations can be also observed. Also, in the right-hand part of the image some cell structures can be also revealed.

The EBIC profiles of individual dislocations measured in the structures A and B are shown in figure 4. It is seen that the FWHM of dislocation EBIC contrast for structure B (150–170 nm) is appreciably smaller than that for structure A (200–240 nm). With such small FWHM values it is possible to resolve individual defects in both structures, even if their density exceeds 10^9 cm^{-2}. The other important observation is that the spatial resolution is improved with increase of primary electron energies E_b, although the decrease of the FWHM with increasing E_b is rather small. As mentioned above, the FWHM in semiconductors with large diffusion length is mainly determined by the generation region dimensions and strongly

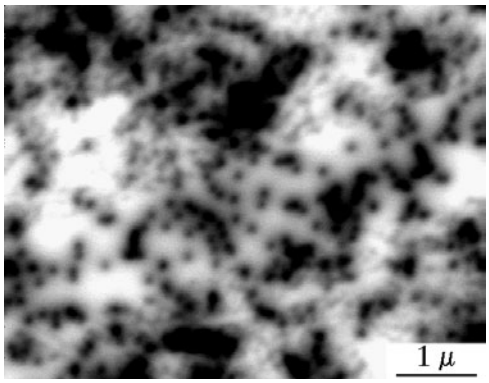

Figure 3. An EBIC image of structure B obtained with higher magnification; $E_b = 35$ keV, $I_b = 3 \times 10^{-10}$ A.

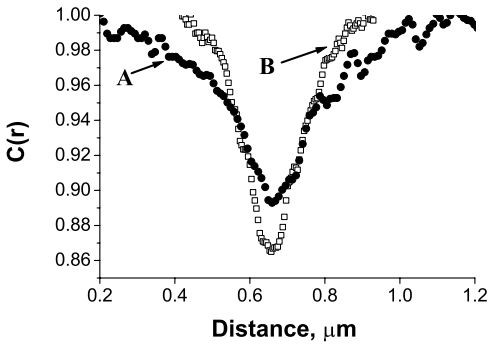

Figure 4. Typical dislocation EBIC profiles obtained for the structures A and B; $E_b = 35$ keV, $I_b = 3 \times 10^{-10}$ A.

increases with E_b. The improvement of spatial resolution in the GaN structures studied can be easily understood under the assumption of a very low diffusion length L_b, which implies a high collection efficiency of excess carriers only in a thin near-surface layer. The generation region width in the near-surface layer decreases with increasing E_b [9] and this leads to the improvement of the spatial resolution in structures with low diffusion length. To check this assumption, the dependence of the collection efficiency on the beam energy was investigated. The collection efficiency was calculated as $I_c/(aI_bE_b)$, where I_c is the current collected by the Schottky barrier under the electron beam excitation, I_b is the electron beam current, $a = E_i/\eta$, E_i is the energy necessary for the creation of an electron–hole pair, and η is the backscattering energy coefficient. Although either of the estimates of the E_i- and η-values could be used for GaN, the coefficient a calculated from our experimental data was found to be rather close to the estimated one. Therefore, the coefficient a was chosen in such a way that the collection efficiency for structure A approaches 1 at small values of E_b.

The dependence of the collection efficiency on E_b measured for the structures A and B is shown in figure 5. In both cases the collection efficiency was averaged over an area of 0.03 mm^2. It could be seen that in structure B the decay of the collection efficiency with the depth is sharper than that in structure A. This observation shows that the average diffusion length L_{eff} in sample B is smaller than that in sample A, in good agreement with the better spatial resolution observed for sample B (figures 1(a), (b) and 4). Figure 5 reports the

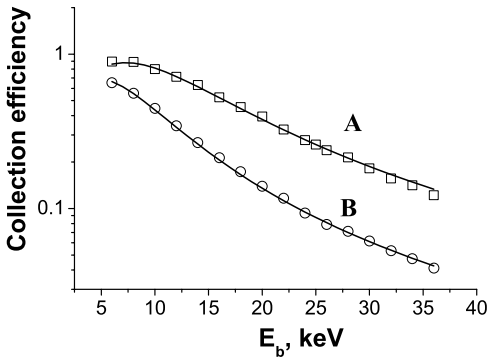

Figure 5. Measured (symbols) and simulated (solid curves) dependences of the collection efficiency on E_b for structures A and B.

dependence of the collection efficiency on E_b calculated using the depth-dependent generation function obtained by a Monte Carlo simulation. It is seen that the curves obtained using L_{eff}-values equal to 0.13 and 0.3 μm for the B and A structures, respectively, fit the experimental dependences very well. It should be noted that L_b-values obtained by fitting the dislocation EBIC profiles presented in figure 4 are very close to the L_{eff}-values, thus indicating that the presence of dislocations results in a small effect on the average diffusion length.

The results presented reveal rather close correlation between the electrical properties of GaN and the density of recombination defects. In fact, an increase in defect density leads to a decrease of both the carrier mobility and L_{eff}. While the decrease of the carrier mobility can be explained by taking it into account that dislocations in n-type GaN are negatively charged [10–12], the question of the dislocation effect on L_{eff} seems to be more complex. Indeed, the dislocation recombination strength γ_d can be obtained by fitting the dislocation EBIC profile and then this parameter can be used for estimating the average diffusion length [13]. Such estimation shows, however, that the difference in average diffusion length between samples A and B should be smaller than that shown in figure 5. This discrepancy could be explained under the assumption that most of the defects revealed in structure B are dislocation clusters, which should show a larger contrast and, thus, have larger values of γ_d.

However, the L_{eff}-values obtained by fitting the collection efficiency dependence on E_b and the L_b-values estimated from the EBIC profile fitting were found to be very close. This conclusion allows us to assume that the change of buffer-layer growth conditions should influence not only the dislocation density, but also the concentration of other non-radiative recombination centres. The DLTS measurements also showed that the total deep-level centre concentration in the upper half of the gap in sample B is larger than that in structure A, although in both structures this concentration is too low to explain the diffusion length values observed.

In conclusion, a deep submicron spatial resolution in the EBIC mode is demonstrated for GaN epilayers. It is shown that the defect density which could be resolved approaches 10^{10} cm^{-2}, comparable with that of routine TEM studies. It is shown that this high spatial resolution is associated with the low diffusion length in the samples under study. It is therefore demonstrated not only that the EBIC is a very promising technique for the characterization of GaN-related materials, but also that it can be used for the study of the properties of individual defects in such materials even in the case where the defect density exceeds 10^9 cm^{-2}.

References

[1] Alexander H 1994 *Mater. Sci. Eng.* B **24** 1
[2] Kittler M and Seifert W 1996 *Mater. Sci. Eng.* B **42** 8
[3] Donolato C 1978/1979 *Optik* **52** 19
[4] Donolato C 1983 *J. Physique* **44** C4 269
[5] Rode D L and Gaskill D K 1995 *Appl. Phys. Lett.* **66** 1972
[6] Goodman S A *et al* 2000 *Mater. Sci. Eng.* B **71** 100
[7] Polyakov A Y *et al* 2000 *MRS Internet J. Nitride Semicond. Res.* **5S1** W11.81
[8] Jain S C, Willander M and Narayan J 2000 *J. Appl. Phys.* **87** 965
[9] Donolato C 1981 *Phys. Status Solidi* a **65** 649
[10] Koley G and Spencer M G 2001 *Appl. Phys. Lett.* **78** 2873
[11] Cherns D and Jiao C G 2001 *Phys. Rev. Lett.* **87** 205504
[12] Farvacque J-L, Bougrioua Z and Moerman I 2001 *Phys. Rev.* B **63** 115202
[13] Donolato C 1998 *J. Appl. Phys.* **84** 2656